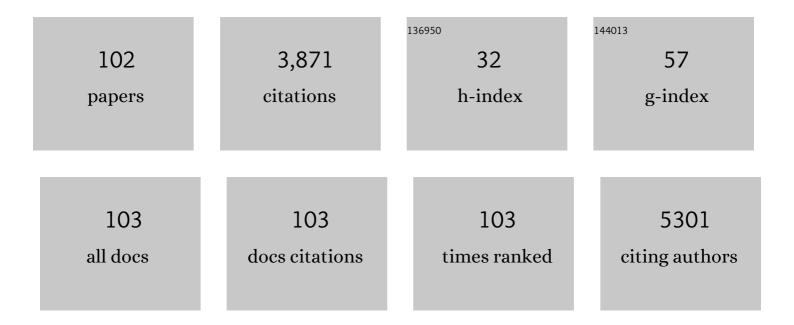
List of Publications by Year in descending order

Source: https://exaly.com/author-pdf/7965926/publications.pdf Version: 2024-02-01



FOV ABOULHAMAD

#	Article	IF	CITATIONS
1	Polytriazole membranes with ultrathin tunable selective layer for crude oil fractionation. Science, 2022, 376, 1105-1110.	12.6	44
2	Rapid fabrication of MOF-based mixed matrix membranes through digital light processing. Materials Advances, 2021, 2, 2739-2749.	5.4	12
3	The Importance of Thermal Treatment on Wet-Kneaded Silica–Magnesia Catalyst and Lebedev Ethanol-to-Butadiene Process. Nanomaterials, 2021, 11, 579.	4.1	5
4	Organic solvent and thermal resistant polytriazole membranes with enhanced mechanical properties cast from solutions in non-toxic solvents. Journal of Membrane Science, 2020, 597, 117634.	8.2	21
5	Aromatization of Ethylene – Main Intermediate for MDA?. ChemCatChem, 2020, 12, 544-549.	3.7	22
6	Acidity modification of ZSM-5 for enhanced production of light olefins from CO2. Journal of Catalysis, 2020, 381, 347-354.	6.2	52
7	Titanium methyl tamed on silica: synthesis of a well-defined pre-catalyst for hydrogenolysis of <i>n</i> -alkane. Chemical Communications, 2020, 56, 13401-13404.	4.1	4
8	Non-oxidative dehydrogenation of isobutane over supported vanadium oxide: nature of the active sites and coke formation. Catalysis Science and Technology, 2020, 10, 6139-6151.	4.1	12
9	Smart covalent organic networks (CONs) with "on-off-on―light-switchable pores for molecular separation. Science Advances, 2020, 6, eabb3188.	10.3	71
10	Impact of small promoter amounts on coke structure in dry reforming of methane over Ni/ZrO ₂ . Catalysis Science and Technology, 2020, 10, 3965-3974.	4.1	27
11	Initial Carbonâ^'Carbon Bond Formation during the Early Stages of Methane Dehydroaromatization. Angewandte Chemie, 2020, 132, 16884.	2.0	3
12	Initial Carbonâ^'Carbon Bond Formation during the Early Stages of Methane Dehydroaromatization. Angewandte Chemie - International Edition, 2020, 59, 16741-16746.	13.8	36
13	Spray-coated graphene oxide hollow fibers for nanofiltration. Journal of Membrane Science, 2020, 606, 118006.	8.2	27
14	Highly Stable Phosphonateâ€Based MOFs with Engineered Bandgaps for Efficient Photocatalytic Hydrogen Production. Advanced Materials, 2020, 32, e1906368.	21.0	117
15	Docking of tetra-methyl zirconium to the surface of silica: a well-defined pre-catalyst for conversion of CO ₂ to cyclic carbonates. Chemical Communications, 2020, 56, 3528-3531.	4.1	16
16	Coated sulfated zirconia/SAPO-34 for the direct conversion of CO ₂ to light olefins. Catalysis Science and Technology, 2020, 10, 1507-1517.	4.1	34
17	The elemental analysis and multi-nuclear NMR study of an alkali molten salt used to digest reference and commercial SWCNT powders. Journal of Analytical Atomic Spectrometry, 2020, 35, 2758-2769.	3.0	1
18	Mechanistic Study of Hydroamination of Alkyne through Tantalum-Based Silica-Supported Surface Species. ACS Catalysis, 2019, 9, 8719-8725.	11.2	15

#	Article	IF	CITATIONS
19	Heterostructured MXene and g-C3N4 for high-rate lithium intercalation. Nano Energy, 2019, 65, 104030.	16.0	54
20	Surface enhanced dynamic nuclear polarization solid-state NMR spectroscopy sheds light on BrÃ,nsted–Lewis acid synergy during the zeolite catalyzed methanol-to-hydrocarbon process. Chemical Science, 2019, 10, 8946-8954.	7.4	30
21	[Cu ₆₁ (S ^t Bu) ₂₆ S ₆ Cl ₆ H ₁₄] ^{+< A Core–Shell Superatom Nanocluster with a Quasi-<i>J</i>₃₆ Cu₁₉ Core and an "18-Crown-6―Metal-Sulfide-like Stabilizing Belt. , 2019, 1, 297-302.}	:/sup>:	76
22	Chemical and Structural Analysis of Carbon Materials Subjected to Alkaline Oxidation. ACS Omega, 2019, 4, 18725-18733.	3.5	4
23	Use of the Phenâ€NaDPO:Sn(SCN) ₂ Blend as Electron Transport Layer Results to Consistent Efficiency Improvements in Organic and Hybrid Perovskite Solar Cells. Advanced Functional Materials, 2019, 29, 1905810.	14.9	41
24	A Supramolecular View on the Cooperative Role of BrÃ,nsted and Lewis Acid Sites in Zeolites for Methanol Conversion. Journal of the American Chemical Society, 2019, 141, 14823-14842.	13.7	80
25	Tetracrystalline Tetrablock Quarterpolymers: Four Different Crystallites under the Same Roof. Angewandte Chemie - International Edition, 2019, 58, 16267-16274.	13.8	13
26	A site-sensitive quasi-in situ strategy to characterize Mo/HZSM-5 during activation. Journal of Catalysis, 2019, 370, 321-331.	6.2	40
27	Quantifying the impact of dispersion, acidity and porosity of Mo/HZSM-5 on the performance in methane dehydroaromatization. Applied Catalysis A: General, 2019, 574, 144-150.	4.3	28
28	Bimetallic Pt-Sn nanocluster from the hydrogenolysis of a well-defined surface compound consisting of [(AlO)Pt(COD)Me] and [(AlO)SnPh3] fragments for propane dehydrogenation. Journal of Catalysis, 2019, 374, 391-400.	6.2	34
29	Effect of Zeolite Topology and Reactor Configuration on the Direct Conversion of CO ₂ to Light Olefins and Aromatics. ACS Catalysis, 2019, 9, 6320-6334.	11.2	144
30	Tandem Conversion of CO ₂ to Valuable Hydrocarbons in Highly Concentrated Potassium Iron Catalysts. ChemCatChem, 2019, 11, 2879-2886.	3.7	57
31	A strategy to convert propane to aromatics (BTX) using TiNp ₄ grafted at the periphery of ZSM-5 by surface organometallic chemistry. Dalton Transactions, 2019, 48, 6611-6620.	3.3	6
32	Tetracrystalline Tetrablock Quarterpolymers: Four Different Crystallites under the Same Roof. Angewandte Chemie, 2019, 131, 16413-16420.	2.0	1
33	TiO ₂ -supported Pt single atoms by surface organometallic chemistry for photocatalytic hydrogen evolution. Physical Chemistry Chemical Physics, 2019, 21, 24429-24440.	2.8	32
34	Extremely Hydrophobic POPs to Access Highly Porous Storage Media and Capturing Agent for Organic Vapors. CheM, 2019, 5, 180-191.	11.7	42
35	Tungsten Catalyst Incorporating a Wellâ€Defined Tetracoordinated Aluminum Surface Ligand for Selective Metathesis of Propane, [(≡Siâ^'Oâ''Si≡)(≡Siâ^'Oâ^') ₂ Alâ^'Oâ^'W(≡C <i>t</i> Bu) (H) ₂]. ChemCatChem, 2019, 11, 614-620.	3.7	2
36	Exploiting the interactions between the ruthenium Hoveyda–Grubbs catalyst and Al-modified mesoporous silica: the case of SBA15 <i>vs.</i> KCC-1. Chemical Science, 2018, 9, 3531-3537.	7.4	18

#	Article	IF	CITATIONS
37	A Silica-Supported Monoalkylated Tungsten Dioxo Complex Catalyst for Olefin Metathesis. ACS Catalysis, 2018, 8, 2715-2729.	11.2	38
38	Clean chlorination of silica surfaces by a single-site substitution approach. Dalton Transactions, 2018, 47, 4301-4306.	3.3	14
39	Predicting the DNP-SENS efficiency in reactive heterogeneous catalysts from hydrophilicity. Chemical Science, 2018, 9, 4866-4872.	7.4	24
40	On the dynamic nature of Mo sites for methane dehydroaromatization. Chemical Science, 2018, 9, 4801-4807.	7.4	65
41	Solventâ€Free Synthesis of Quaternary Metal Sulfide Nanoparticles Derived from Thiourea. Particle and Particle Systems Characterization, 2018, 35, 1700183.	2.3	7
42	Recognizing the Mechanism of Sulfurized Polyacrylonitrile Cathode Materials for Li–S Batteries and beyond in Al–S Batteries. ACS Energy Letters, 2018, 3, 2899-2907.	17.4	224
43	Synthesis and Characterization of Cationic Tetramethyl Tantalum(V) Complex. Catalysts, 2018, 8, 507.	3.5	1
44	Imine Metathesis Catalyzed by a Silica-Supported Hafnium Imido Complex. ACS Catalysis, 2018, 8, 9440-9446.	11.2	20
45	Morphology control of anatase TiO2 for well-defined surface chemistry. Physical Chemistry Chemical Physics, 2018, 20, 14362-14373.	2.8	25
46	Structure–performance descriptors and the role of Lewis acidity in the methanol-to-propylene process. Nature Chemistry, 2018, 10, 804-812.	13.6	221
47	Benzimidazole linked polymers (BILPs) in mixed-matrix membranes: Influence of filler porosity on the CO2/N2 separation performance. Journal of Membrane Science, 2018, 566, 213-222.	8.2	20
48	SOMC grafting of vanadium oxytriisopropoxide (VO(O ⁱ Pr) ₃) on dehydroxylated silica; analysis of surface complexes and thermal restructuring mechanism. RSC Advances, 2018, 8, 20801-20808.	3.6	11
49	Unearthing a Well-Defined Highly Active Bimetallic W/Ti Precatalyst Anchored on a Single Silica Surface for Metathesis of Propane. Journal of the American Chemical Society, 2017, 139, 3522-3527.	13.7	30
50	Hybrid electrolytes based on ionic liquids and amorphous porous silicon nanoparticles: Organization and electrochemical properties. Applied Materials Today, 2017, 9, 10-20.	4.3	16
51	Single site silica supported tetramethyl niobium by the SOMC strategy: synthesis, characterization and structure–activity relationship in the ethylene oligomerization reaction. Chemical Communications, 2017, 53, 7068-7071.	4.1	9
52	From single-site tantalum complexes to nanoparticles of Ta _x N _y and TaO _x N _y supported on silica: elucidation of synthesis chemistry by dynamic nuclear polarization surface enhanced NMR spectroscopy and X-ray absorption spectroscopy. Chemical Science, 2017, 8, 5650-5661.	7.4	14
53	Conversion of actual flue gas CO 2 via cycloaddition to propylene oxide catalyzed by a single-site, recyclable zirconium catalyst. Journal of CO2 Utilization, 2017, 20, 243-252.	6.8	60
54	The structure and binding mode of citrate in the stabilization of gold nanoparticles. Nature Chemistry, 2017, 9, 890-895.	13.6	222

#	Article	IF	CITATIONS
55	Well-Defined Silica Grafted Molybdenum Bis(imido) Catalysts for Imine Metathesis Reactions. Organometallics, 2017, 36, 1550-1556.	2.3	12
56	Synthesis of single-crystal-like nanoporous carbon membranes and their application in overall water splitting. Nature Communications, 2017, 8, 13592.	12.8	142
57	SOMC-Designed Silica Supported Tungsten Oxo Imidazolin-2-iminato Methyl Precatalyst for Olefin Metathesis Reactions. Inorganic Chemistry, 2017, 56, 861-871.	4.0	23
58	Reactive surface organometallic complexes observed using dynamic nuclear polarization surface enhanced NMR spectroscopy. Chemical Science, 2017, 8, 284-290.	7.4	55
59	Cationic Tungsten(VI) Penta-Methyl Complex: Synthesis, Characterization and its Application in Olefin Metathesis Reaction. Oil and Gas Science and Technology, 2016, 71, 21.	1.4	2
60	Single-Site Tetracoordinated Aluminum Hydride Supported on Mesoporous Silica. From Dream to Reality!. Organometallics, 2016, 35, 3288-3294.	2.3	17
61	Tungsten(VI) Carbyne/Bis(carbene) Tautomerization Enabled by Nâ€Đonor SBA15 Surface Ligands: A Solidâ€State NMR and DFT Study. Angewandte Chemie - International Edition, 2016, 55, 11162-11166.	13.8	13
62	Single-Site VO _{<i>x</i>} Moieties Generated on Silica by Surface Organometallic Chemistry: A Way To Enhance the Catalytic Activity in the Oxidative Dehydrogenation of Propane. ACS Catalysis, 2016, 6, 5908-5921.	11.2	74
63	Investigation of Surface Alkylation Strategy in SOMC: In Situ Generation of a Silica-Supported Tungsten Methyl Catalyst for Cyclooctane Metathesis. Organometallics, 2016, 35, 2524-2531.	2.3	4
64	Synthesis and characterization of a homogeneous and silica supported homoleptic cationic tungsten(<scp>vi</scp>) methyl complex: application in olefin metathesis. Chemical Communications, 2016, 52, 11270-11273.	4.1	10
65	Solidâ€State NMR and DFT Studies on the Formation of Wellâ€Defined Silicaâ€Supported Tantallaaziridines: From Synthesis to Catalytic Application. Chemistry - A European Journal, 2016, 22, 3000-3008.	3.3	18
66	Atomic-level organization of vicinal acid–base pairs through the chemisorption of aniline and derivatives onto mesoporous SBA15. Chemical Science, 2016, 7, 6099-6105.	7.4	16
67	Synergy between Two Metal Catalysts: A Highly Active Silica-Supported Bimetallic W/Zr Catalyst for Metathesis of <i>n</i> -Decane. Journal of the American Chemical Society, 2016, 138, 8595-8602.	13.7	34
68	CO ₂ activation through silylimido and silylamido zirconium hydrides supported on N-donor chelating SBA15 surface ligands. Chemical Communications, 2016, 52, 2577-2580.	4.1	10
69	Controlling the hydrogenolysis of silica-supported tungsten pentamethyl leads to a class of highly electron deficient partially alkylated metal hydrides. Chemical Science, 2016, 7, 1558-1568.	7.4	53
70	Organosilane with Gemini-Type Structure as the Mesoporogen for the Synthesis of the Hierarchical Porous ZSM-5 Zeolite. Langmuir, 2016, 32, 2085-2092.	3.5	21
71	Well-defined silica-supported zirconium–imido complexes mediated heterogeneous imine metathesis. Chemical Communications, 2016, 52, 4617-4620.	4.1	26
72	Wellâ€Defined Singleâ€Site Monohydride Silicaâ€Supported Zirconium from Azazirconacyclopropane. Chemistry - A European Journal, 2015, 21, 4294-4299.	3.3	15

#	Article	IF	CITATIONS
73	Isolation and Characterization of Wellâ€Defined Silicaâ€Supported Azametallacyclopentane: A Key Intermediate in Catalytic Hydroaminoalkylation Reactions. Advanced Synthesis and Catalysis, 2015, 357, 3148-3154.	4.3	26
74	Alkane Metathesis with the Tantalum Methylidene [(≡SiO)Ta(â•CH ₂)Me ₂]/[(≡SiO) ₂ Ta(â•CH ₂)Me] Generat from Well-Defined Surface Organometallic Complex [(≡SiO)Ta ^V Me ₄]. Journal of the American Chemical Society, 2015, 137, 588-591.	red 13.7	65
75	Well-defined silica supported aluminum hydride: another step towards the utopian single site dream?. Chemical Science, 2015, 6, 5456-5465.	7.4	22
76	Room-Temperature Reactivity Of Silicon Nanocrystals With Solvents: The Case Of Ketone And Hydrogen Production From Secondary Alcohols: Catalysis?. ACS Applied Materials & Interfaces, 2015, 7, 13794-13800.	8.0	19
77	Rigid, non-porous and tunable hybrid p-aminobenzoate/TiO2 materials: Toward a fine structural determination of the immobilized RhCl(Ph3)3 complex. Journal of Organometallic Chemistry, 2015, 784, 103-108.	1.8	1
78	Cooperative Effect of Monopodal Silica-Supported Niobium Complex Pairs Enhancing Catalytic Cyclic Carbonate Production. Journal of the American Chemical Society, 2015, 137, 7728-7739.	13.7	123
79	Effect of Support on Metathesis of <i>n</i> â€Decane: Drastic Improvement in Alkane Metathesis with WMe ₅ Linked to Silica–Alumina. Chemistry - A European Journal, 2015, 21, 6100-6106.	3.3	27
80	Well-Defined Surface Species [(≡Si—O—)W(â•O)Me ₃] Prepared by Direct Methylation of [(≡Si—O—)W(â•O)Cl ₃], a Catalyst for Cycloalkane Metathesis and Transformation of Ethylene to Propylene. ACS Catalysis, 2015, 5, 2164-2171.	11.2	35
81	Direct Functionalization of Nanodiamonds with Maleimide. Chemistry of Materials, 2014, 26, 2766-2769.	6.7	25
82	Sn surface-enriched Pt–Sn bimetallic nanoparticles as a selective and stable catalyst for propane dehydrogenation. Journal of Catalysis, 2014, 320, 52-62.	6.2	144
83	The use of a well-defined surface organometallic complex as a probe molecule: [(ĩ€,SiO)Ta ^V Cl ₂ Me ₂] shows different isolated silanol sites on the silica surface. Chemical Communications, 2014, 50, 11721-11723.	4.1	2
84	Low temperature activation of methane over a zinc-exchanged heteropolyacid as an entry to its selective oxidation to methanol and acetic acid. Chemical Communications, 2014, 50, 12348-12351.	4.1	22
85	WMe6 Tamed by Silica: ≡Si–O–WMe5 as an Efficient, Well-Defined Species for Alkane Metathesis, Leading to the Observation of a Supported W–Methyl/Methylidyne Species. Journal of the American Chemical Society, 2014, 136, 1054-1061.	13.7	84
86	Facile and Efficient Synthesis of the Surface Tantalum Hydride (≡SiO) ₂ Ta ^{III} H and Tris-Siloxy Tantalum (≡SiO) ₃ Ta ^{III} Starting from Novel Tantalum Surface Species (≡SiO)TaMe ₄ and (≡SiO) ₂ TaMe ₃ . Organometallics, 2014, 3: 1205-1211.	3 ^{2.3}	22
87	Well-defined mono(η3-allyl)nickel complex î€,MONi(η3-C3H5) (M = Si or Al) grafted onto silica or alumina: a	4.1	12
88	Bipodal Surface Organometallic Complexes with Surface N-Donor Ligands and Application to the Catalytic Cleavage of C–H and C–C Bonds in n-Butane. Journal of the American Chemical Society, 2013, 135, 17943-17951.	13.7	33
89	Well-defined azazirconacyclopropane complexes supported on silica structurally determined by 2D NMR comparative elucidation. Chemical Communications, 2013, 49, 4616.	4.1	20
90	Methane Reacts with Heteropolyacids Chemisorbed on Silica to Produce Acetic Acid under Soft Conditions. Journal of the American Chemical Society, 2013, 135, 804-810.	13.7	24

#	Article	IF	CITATIONS
91	[(SiO)TaV(CH2)Cl2], the first tantalum methylidene species prepared and identified on the silica surface. Journal of Organometallic Chemistry, 2013, 744, 3-6.	1.8	9
92	Electromagnetic Properties of Inner Double Walled Carbon Nanotubes Investigated by Nuclear Magnetic Resonance. Journal of Nanomaterials, 2013, 2013, 1-6.	2.7	3
93	[(SiO)Ta ^V Cl ₂ Me ₂]: A Wellâ€Defined Silicaâ€Supported Tantalum(V) Surface Complex as Catalyst Precursor for the Selective Cocatalystâ€Free Trimerization of Ethylene. Angewandte Chemie - International Edition, 2012, 51, 11886-11889.	13.8	45
94	A Silica-Supported Double-Decker Silsesquioxane Provides a Second Skin for the Selective Generation of Bipodal Surface Organometallic Complexes. Organometallics, 2012, 31, 7610-7617.	2.3	22
95	A well-defined mesoporous amine silica surface via a selective treatment of SBA-15 with ammonia. Chemical Communications, 2012, 48, 3067.	4.1	25
96	Carbon nanotubes and helical carbon nanofibers grown by chemical vapour deposition on C60 fullerene supported Pd nanoparticles. Carbon, 2011, 49, 1101-1107.	10.3	44
97	Confined adamantane molecules assembled to one dimension in carbon nanotubes. Carbon, 2011, 49, 1159-1166.	10.3	24
98	Hydrogenation of C ₆₀ in Peapods: Physical Chemistry in Nano Vessels. Journal of Physical Chemistry C, 2009, 113, 8583-8587.	3.1	29
99	One-step electrochemical modification of carbon nanotubes by ruthenium complexes via new diazonium salts. Journal of Electroanalytical Chemistry, 2008, 621, 277-285.	3.8	64
100	High-Purity Diamagnetic Single-Wall Carbon Nanotube Buckypaper. Chemistry of Materials, 2007, 19, 2982-2986.	6.7	39
101	Routes to the synthesis of carbon nanotube–polyacetylene composites by Ziegler–Natta polymerization of acetylene inside carbon nanotubes. Current Applied Physics, 2007, 7, 39-41.	2.4	29
102	Polymerization of conducting polymers inside carbon nanotubes. Chemical Physics Letters, 2006, 431, 139-144.	2.6	41